International Journal of Pharmaceutics 668 (2025) 124967

Contents lists available at ScienceDirect

International Journal of Pharmaceutics

journal homepage: www.elsevier.com/locate/ijpharm

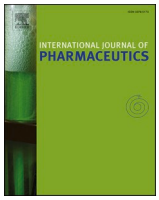

Machine learning strengthened formulation design of pharmaceutical suspensions

Nadina Zulbeari [a,1], Fanjin Wang [b,1], Sibel Selyatinova Mustafova [a], Maryam Parhizkar [b], René Holm [a,*]

[a] Department of Physics, Chemistry, and Pharmacy, University of Southern Denmark, Campusvej 55, 5230 Odense, Denmark
[b] Deparment of Pharmaceutics, UCL School of Pharmacy, University College London, 29-39 Brunswick Square, WC1N 1AX London, United Kingdom

ARTICLE INFO

Keywords:
Stabilizers
Formulation screening
Nano
Microsuspensions
Machine learning

ABSTRACT

Many different formulation strategies have been investigated to oppose suboptimal treatment of long-term or chronic conditions, one of which are the nano- and microsuspensions prepared as long-acting injectables to prolong the release of an active pharmaceutical compound for a defined period of time by regulating the size of particles by milling. Typically, surfactant and/or polymers are added in the dispersion medium of the suspension during processing for stabilization purposes. However, current formulation investigations with milling are heavily based on prior expertise and trial-and-error approaches. Various interacting parameters such as the milling bead size, stabilizer type and concentration have confounded the investigation of milling process. The present study systematically exploited statistical and machine learning (ML) strategies to understand the relationship between suspension characteristics and formulation parameters under full-factorial milling experiments. Stabilizer concentration was identified as a significant factor ($p < 0.001$) for median suspension diameter (D_{50}). A formulation stability classification ML model with high prediction accuracy (0.91) and F1-score (0.91) under 10-fold cross-validation was constructed based on 72 formulation datapoints. Model interpretation through Shapley additive explanations (SHAP) revealed the prominent impact of stabilizer concentration and milling bead size on formulation stability. The present work demonstrated the potential to achieve a deeper understanding of the design and optimization of nano- and microsuspensions through explainable ML modelling on formulation screening data.

1. Introduction

To overcome suboptimal treatment outcome of long-term or chronic conditions (*e.g.,* schizophrenia or human immunodeficiency virus (HIV)) and poor patient compliance due to frequent administration, several formulation strategies have been investigated (Park et al., 2013; Okoli et al., 2022). Among these, long-acting injectables (LAIs) have clinically been shown to prolong the release of an active pharmaceutical compound for weeks to months by a single injection. LAIs are based on different formulation techniques, where aqueous suspensions containing crystalline drug particles can be engineered to release the active compound for a predefined plasma-concentration profile, within a safe therapeutic range, by controlling the sizes of the drug particles (Park et al., 2013; Owen & Rannard, 2016; Pacchiarotti et al., 2019; Nkanga et al., 2020; Bao et al., 2021; Okoli et al., 2022; Wilkinson et al., 2022; Bauer et al., 2023; Holm et al., 2023; Alidori et al., 2024).

The manufacturing of nano- and microsuspensions is often prepared by the highly efficient wet bead media milling (*i.e.,* top-down size reduction approach) which reduces the size of larger drug particles into smaller particles by the friction from mechanical forces generated by milling beads while suspended in an aqueous stabilizer vehicle (Verma et al., 2009; Nakach et al., 2014; Mishra et al., 2015; Hagedorn et al., 2017; Willmann et al., 2022; Guner et al., 2023). However, a common attribute of disperse systems is the unstable thermodynamics which ultimately can affect the long-term stability (Kipp, 2004; Azad et al., 2015; Nakach et al., 2016; Holm et al., 2023). Nano- and microsuspensions must therefore be formulated to overcome stability challenges such as agglomeration or crystal growth by Ostwald ripening. Stabilizers in the form of surfactants and/or polymers are therefore essential contributors due to their ability to prevent inter-particle forces by electrostatic

* Corresponding author.
E-mail address: reho@sdu.dk (R. Holm).
[1] Both authors have contributed equally and are considered co-first authors.

https://doi.org/10.1016/j.ijpharm.2024.124967
Received 14 September 2024; Received in revised form 15 November 2024; Accepted 16 November 2024
Available online 19 November 2024

repulsion and/or steric stabilization (Peltonen & Hirvonen, 2010; Verma et al., 2011; Nakach et al., 2014; Lestari et al., 2015; Willmann et al., 2022; Holm et al., 2023). Thus, the selection of stabilizer and adequate concentration is highly dependent on the specific formulation and the drug compounds physical–chemical properties with various factors in mind such as the surfactant adsorption and affinity for the drug particle surface (Peltonen & Hirvonen, 2010; Nakach et al., 2014). The screening of proper stabilization compositions for pharmaceutical suspensions is therefore currently based on a time-consuming trial and error approach (Peltonen & Hirvonen, 2010) with previous studies emphasizing on the impact of formulation parameters (*e.g.,* stabilizers) on the physical attributes of the final suspensions (Bitterlich et al., 2015; Ferrar et al., 2020; Karakucuk & Celebi, 2020; Willmann et al., 2022).

To define the optimal formulation design of pharmaceutical suspensions can be a complex and time-consuming barrier due to the comprehensive screening of optimal stabilizer composition, but nevertheless crucial for the preparation of a well-functioning LAIs with superior long-term stability. Only few studies in the literature have focused on the selection of stabilizers for the preparation of nano- and microsuspensions to strengthen the formulation design (Choi et al., 2005; Lee et al., 2008; Van Eerdenbrugh et al., 2009; Nakach et al., 2014; Lestari et al., 2015). However, most studies placed emphasis on empirical research relying on experimental screening data or the formulation characteristics such as the physicochemical properties (Nakach et al., 2014). For instance, two different studies by Van Eerdenbrugh et al. 2009 and Lestari et al. 2015 performed screening studies on a number of different structural stabilizers in various concentrations to investigate the importance of suitable stabilizers with respect to the physical stability of nanosuspensions. The studies reported some general correlations and showed that a higher stabilization concentration showed positive stabilization effect during suspension preparation. A study by Nakach and coworkers (Nakach et al., 2014) instead proposed a stepwise screening approach based on the compounds physicochemical properties to select an optimum stabilizing agent. Similarly, George and Ghosh (2013) proposed key drug properties that had a direct outcome on the formation of stable nanosuspensions as for instance the degree of hydrophobicity investigating in total six different compounds (George & Ghosh, 2013). Another screening approach was based on the surface energies between the stabilizers and the drug compound presented by Choi et al. 2005 and Lee et al. 2008. More recently, a study by Zulbeari and colleagues (Zulbeari et al., 2024) investigated the correlation between the surface activity of two different surfactants and obtained particle size profiles after milling by dual centrifugation to predict a suitable stabilization concentration based upon short-term stress physical stability data.

Formulating suspensions provides a complex dataset that is judged by the formulator to identify the most optimal suspension. Another interesting formulation optimization approach for suspensions could be the application of machine learning (ML). The development of ML has in recent years has advanced pharmaceutics research, including drug discovery and development, for modelling and optimization purposes of pharmaceutical formulations (Vamathevan et al., 2019; Bannigan et al., 2021; Wang et al., 2022). For example, Bannigan *et al.* extracted data from 29 previous publications and obtained a dataset consisting of 181 drug release profiles, providing ML models to predict the release behaviors of LAIs (Bannigan et al., 2023). However, many critical aspects in formulation design, such as drug compound compatibility and storage stability, were not fully investigated using ML, since the limited availability of open-source datasets and experiment reports (Bannigan et al., 2023). The present study investigated a full-factorial design data consisting of an existing formulation screening result of two surfactants polysorbate 20 and poloxamer 188 (Zulbeari et al., 2024) and a new dataset showing the combinatorial effect of the two stabilizers. The three datasets all relate to the formulation of cinnarizine suspensions, with cinnarizine serving as the model compound. These suspensions were processed using dual centrifugation as the method for milling. Statistical methods were leveraged to provide insights about how formulation parameters could affect the stabilization of prepared suspensions. Finally, explainable ML models were constructed to predict the stability of these formulations based on these parameters.

2. Material and methods

2.1. Materials

Cinnarizine was provided by Janssen Pharmaceutica (Beerse, Belgium). As stabilizers, poloxamer 188 (Thermo Scientific, Kandel, Germany) and polysorbate 20 (Fisher Scientific, Geel, Belgium) were purchased. Sodium phosphate monobasic anhydrous was purchased from VWR Chemicals LLC (Solon, Ohio, USA) to prepare the buffer solution. Zirconium oxide milling beads, stabilized with high-end yttria, were purchased from NETZSCH (VitaBeads® Nano; ø 0.5, 0.8, 1.0 mm, Selb, Germany).

2.2. Milling by the dual centrifugation approach

For sample preparation, 2 mL micro twist-tubes were filled with 100 mg cinnarizine, 1 g milling beads (ø 0.5, 0.8, or 1.0 mm), and 1 mL stabilizer solution containing either poloxamer 188, polysorbate 20, or a mixture of both surfactants. To prepare the stabilizer solutions, the surfactants were dissolved in 50 mM phosphate buffer (pH 7.4) in eight different concentrations that ranged from 0.25 % to 4.00 % (w/v).

The suspensions were milled by the dual centrifugation approach using a DeltaVita 1 (NETZSCH, Selb, Germany) dual centrifuge. A single milling cycle was set to 90 min at 1500 rpm with a rotor temperature set to 0 °C (Hagedorn et al., 2017). For short-term physical stability analysis, the prepared suspensions were separated from the milling beads and stored in closed glass vials at 40 °C until particle size measurements performed after 0, 7, 14, 21, and 28 days of storage.

2.3. Particle size measurements

Sizes of cinnarizine particles were determined by laser diffraction using a Mastersizer 3000 (Malvern Instruments, Malvern, United Kingdom) after 0, 7, 14, 21, and 28 days of suspension storage. The laser diffractometer was connected to a hydro medium volume unit, connected to water that worked as the wet dispersion unit. The stirring rate was set to 1200 rpm during sample measurements and the refractive index of water was set to 1.33. The optical parameters of cinnarizine were adjusted to a refractive index of 1.63 with an absorption index set to 0.1, and a particle density of 1.13 g/cm^3 (De Cleyn et al., 2019; Zulbeari et al., 2024). Each suspension was measured five times.

A volume-based diameter approach based on the Mie-Theory for non-spherical particles were used to interpret the sizes of cinnarizine particles (*d*-values), corresponding particle size distributions, and span. If air bubbles interfered with the obtained particle sizes, the particle size profiles were reanalyzed to exclude those from the measurements (De Cleyn et al., 2019).

2.4. Preliminary data exploration

The suspension data determined by laser diffraction was manually curated in a tabular format consisting of the experiment variables and the results. Variables such as bead size, type of stabilizer, concentration of the stabilizer, and the date after production was collected. Results including D_{10}, D_{50}, and D_{90}, were appended to the corresponding experiment variables. In order to characterize the polydispersity of processed particles, the span of each investigated suspension was calculated by equation (1).

$$Span = \frac{D_{90} - D_{10}}{D_{50}} \quad (1)$$

Distribution plots were generated to explore the evolution of size distribution over days, with respect to the bead size, type of stabilizer, and concentration of the stabilizer. The visualization was produced by Python library Seaborn (version 0.11.2). Two-way ANOVA tests on repeated measurements, under Greenhouse-Geisser correction, were performed to investigate the statistical significance of various parameters. Two-tailed t-tests with Bonferroni correction were performed for the pair-wise comparisons between individual experiment variables. These statistical tests were implemented through OriginPro 2021b software (OriginLab Corporation, United States).

2.5. Quantifying suspension stability

To quantify the stability of the prepared suspensions, four statistics, the mean and standard deviation of both D_{50} and *Span*, were calculated from results of day 0, 7, 14, 21, and 28. Pairwise scatter plots and histograms were obtained though the library Seaborn (version 0.11.2). Furthermore, box plots were leveraged to visualize the relationship between the stability statistics and the respective three formulation variables (bead size, type of stabilizer, concentration of the stabilizer). Finally, the stable zone of suspensions was coined through the quadrants from the scatter plot of the standard deviation of D_{50} and the standard deviation of the span. The kernel density estimation (KDE) and histograms of the scatter plot were visualized to help the identification of the cut-offs. In addition, unsupervised learning strategies, including K-Means clustering and Gaussian mixture models (GMM), were constructed to automatically find clusters (n = 4) from the scatter plot data. The stable/unstable zones defined through unsupervised learning algorithms were compared to the manually cut-offs from the histogram with Cohen's Kappa as an inter-voter metric. These were implemented with Sci-kit learn library (v1.3.0).

2.6. Machine learning model development

Based on the definition of stability, formulations were classified into two categories: stable and unstable. The whole dataset (N = 72) was used for ML modelling with type of stabilizer, concentration of stabilizer, and bead size as the input features. Notably, the type of stabilizer was one-hot encoded with P (for poloxamer 188), P20 (for polysorbate 20), and P + P20 and had been treated as three different stabilizers. The raw values of the other two features were subjected to ML modelling without further preprocessing. The stability was set as the classification target.

Initially, eight ML algorithms were benchmarked to identify the most suitable model, including Support Vector Classification (SVC), Logistic Regression (LR), Random Forest (RF), XGBoost, Light Gradient Boosting Machine (LGBM), Multilayer Perceptron (MLP), k-Nearest Neighbors (kNN), and Gaussian Process (GP). The XGBoost model was implemented with py-xgboost library (v1.7.3), and LGBM used lightgbm Python library (v3.3.5). The other six models were implemented through Scikit-learn library (v1.3.0).

These models went through hyperparameter optimization *via* grid search under 10-fold cross validation. With accuracy as the metric, this process allowed identification of best-performed models under each algorithm. The search space was selected based on recommendations from Scikit-learn library and previous literature to cover a reasonable range of hyperparameters (Table 1).

Classification algorithms with optimized hyperparameters (Table 2) were subjected to benchmarking, where 10-fold cross validation with both accuracy and F_1-score were referenced as evaluation metrics. Here, accuracy and F_1-score were defined by Eq. (2) and Eq (3), respectively,

$$Accuracy = \frac{TP + TN}{TP + TN + FP + FN} \tag{2}$$

Table 1
Hyperparameter search space.

Model	Hyperparameter	Values
SVC	C	[1e-2, 1e-1, 1, 10, 100, 200, 400, 600, 800]
	kernel	['poly', 'rbf']
LR	C	[1, 0.9, 0.8, 0.6]
RF	N_estimator	[50, 100, 200, 500, 700]
	Max_features	['auto', 'sqrt']
	Max_depth	[3, 5, 7, 10]
	Min_samples_split	[2, 5, 8, 10, 12]
	Min_samples_leaf	[1, 3, 5]
XGBoost	Learning_rate	[0.01, 0.1]
	Max_depth	[3, 5, 7, 10]
	Min_child_weight	[1, 3, 5]
	Subsample	[0.5, 0.7]
	Colsample_bytree	[0.5, 0.7]
	N_estimators	[50, 100, 200, 500, 700]
	Reg_lambda	[1.1, 1.5, 2, 4]
LGBM	Learning_rate	[0.01, 0.1]
	Num_leaves	[7, 31, 70, 127]
	Max_depth	[3, 5, 7, 10]
	Min_child_weight	[1, 3, 5]
	Subsample	[0.5, 0.7]
	Colsample_bytree	[0.5, 0.7]
	N_estimators	[50, 100, 200, 500, 700]
	Reg_lambda	[1.1, 1.5, 2, 4]
MLP	Hidden_layer_sizes	[(5, 2), (10, 2), (15, 2)]
kNN	N_neighbors	[3, 5, 7, 9, 11, 13, 15]
GP	kernel	['rbf', 'dotproduct']
	Length scale (for rbf)	[0.1, 1, 10]
	Sigma_0 (for dot product)	[0.1, 1, 10]

Table 2
Optimized hyperparameters.

Model	Hyperparameter	Values
SVC	C	10
	kernel	'poly'
LR	C	1
RF	N_estimator	100
	Max_features	'sqrt'
	Max_depth	5
	Min_samples_split	2
	Min_samples_leaf	1
XGBoost	Learning_rate	0.1
	Max_depth	3
	Min_child_weight	1
	Subsample	0.5
	Colsample_bytree	0.5
	N_estimators	100
	Reg_lambda	1.1
LGBM	Learning_rate	0.1
	Num_leaves	7
	Max_depth	3
	Min_child_weight	1
	Subsample	0.5
	Colsample_bytree	0.5
	N_estimators	500
	Reg_lambda	1.1
MLP	Hidden_layer_sizes	(15, 2)
kNN	N_neighbors	3
GP	kernel	'dotproduct'
	Sigma_0 (for dot product)	0.1

$$F_1 = \frac{2 \bullet TP}{2 \bullet TP + FP + FN} \tag{3}$$

where *TP*, *TN*, *FP*, and *FN* were true positives, true negatives, false positives, and false negatives, respectively. Hyperparameter optimization, modeling training, and model benchmarking were all implemented through Sci-kit learn library (v1.3.0).

Finally, the classification results of models with the highest accuracy and F_1 score were further analyzed through plotting out the confusion

matrix, under a randomly shuffled training/test set partitioning at a ratio of 67 %/33 %. The feature importance and prediction strategy were further explained through SHapley Additive exPlanations (SHAP, v0.42.1). All previous procedures were performed on a PC (i7-11850H, 32 GB memory) within a Conda environment (Python 3.9.17).

3. Results and discussion

3.1. Particle size distribution

Before implementing ML, a qualitative exploration was performed on the dataset to understand the relationship between particle size distribution and the two variables in the experiment: stabilizer type and stabilizer concentration. Notably, the datasets used in the present study were based on an experimental dataset (Zulbeari et al., 2024) which investigated the optimum stabilizer concentration of two different surfactants independently, *i.e.,* poloxamer 188 and polysorbate 20 based on their surface activities, and a new experimental dataset which intended to combine the two surfactants to obtain physical stable nano- and microsuspensions using cinnarizine as the model compound. At first, the obtained volume densities of suspensions prepared using beads of 1.0 mm size were plotted on Fig. 1 (detailed volume distribution plots can be found in Figure S1). Similarly, size distributions of the suspensions milled with the two other beads sizes (ø 0.5 and 0.8 mm) were provided in the Supplementary Materials (Figure S2 and S3). It was inferred from Fig. 1 that suspensions prepared with lower concentrations of stabilizers (in all three cases), displayed a bimodal distribution at the beginning (represented as solid lines, day 0) when milled under the specified conditions. For example, when poloxamer was used as the stabilizer, two peaks were seen around both 0.7 and 2 μm, even for the highest stabilizer concentration (4.00 %).

Both poloxamer 188 and polysorbate 20 are commonly used surfactants for stabilization purposes of suspensions and regulatory accepted for intramuscular injections (Muller & Keck, 2004; Peltonen & Hirvonen, 2010; Food and Administration, 2024), yet the obtained results demonstrated that different amounts of poloxamer 188 and polysorbate 20 were necessary to manufacture stable suspensions, since different particle size profiles of cinnarizine were achieved when investigated under similar process and formulation conditions. In general, a wider distribution, *i.e.,* span, was observed for suspensions stabilized with poloxamer 188 (Fig. 1) with a bimodal distribution with two similar peaks in size, whereas the distribution was slightly narrower when stabilized with polysorbate 20. A wider span in general would most likely result in crystal growth by Ostwald ripening which often occurs in polydisperse systems, where large particles grow at the expense of smaller particles (Holm et al., 2023). A high affinity of the stabilizer for the specific drug particle surface is also a crucial factor to consider (Peltonen & Hirvonen, 2010) since the final particle size and physical stability performance is defined by the formulation design. In most cases, poor choice of stabilizer cannot prevent particle aggregation, whereas an excess of stabilizer unbound to the drug particle surface from a high surfactant concentration or poor drug affinity could promote the rate of Ostwald ripening from solubilized drug particles and lead to unstable formulations (Li et al., 2016).

From a different perspective, the distribution of particles under various concentrations of stabilizers was revealed in Fig. 2. A clear trend was observed, namely that the concentration of stabilizers was positively related to the stabilization of particles over the experiment periods, which was characterized by a narrower span and span variation over time for all three stabilization compositions (*i.e.*, polysorbate 20,

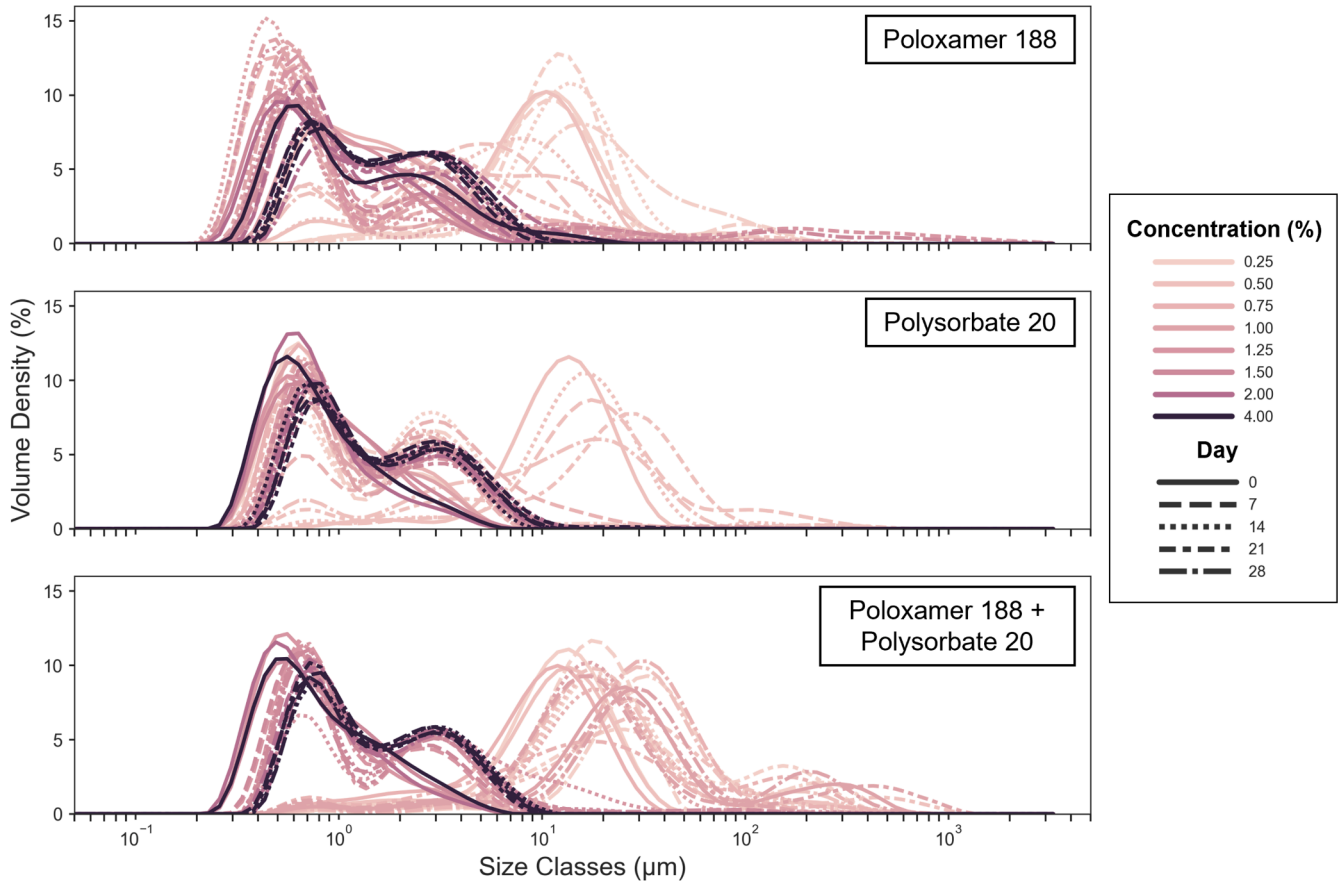

Fig. 1. Particle size distribution of suspensions processed using 1.0 mm beads over 28 days, partitioned on stabilizer type. Formulations prepared with eight different stabilizer concentrations that ranged from 0.25 % to 4.00 % (w/v) were color-coded. Line types represent the results tested on various days after preparation.

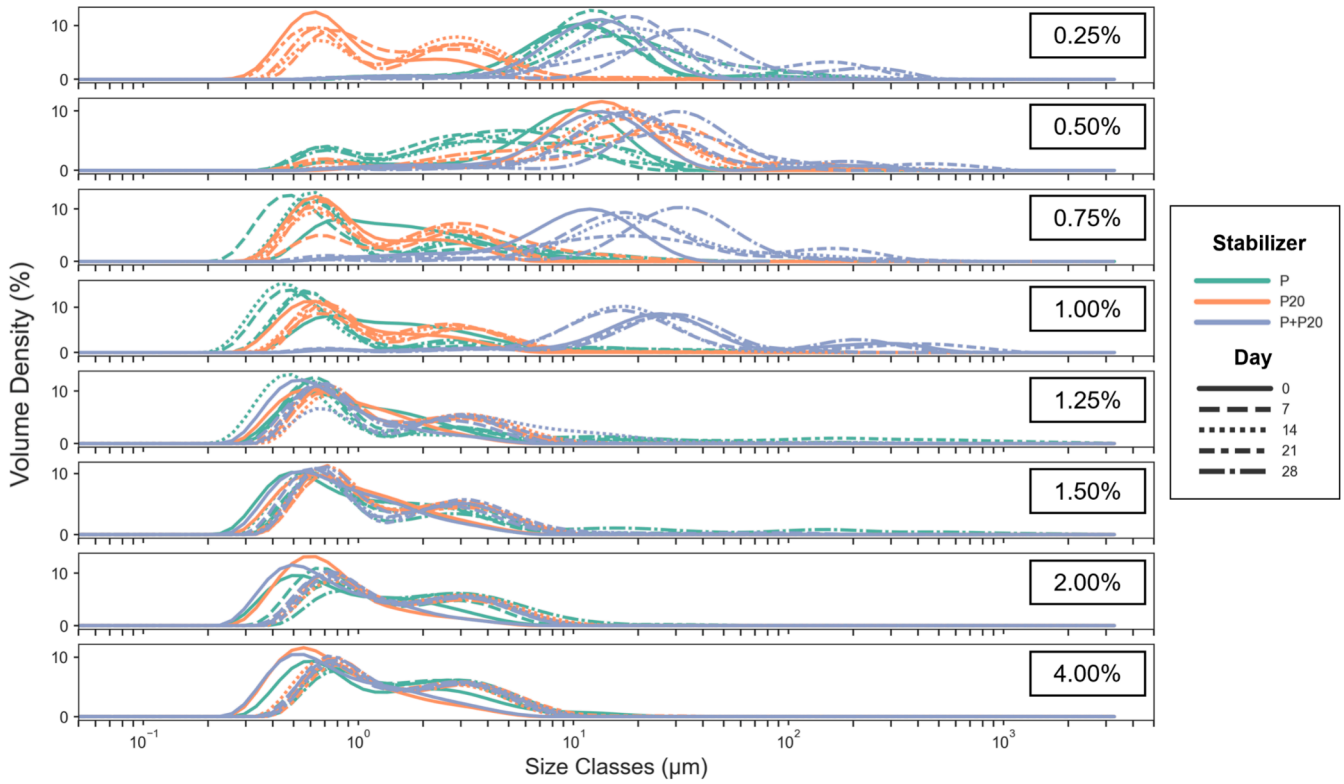

Fig. 2. Particle size distribution of suspensions processed using 1.0 mm beads over 28 days after storage at 40 °C, partitioned on stabilizer concentration which ranged from 0.25 % to 4.00 % (w/v). Formulations prepared with different stabilizers (P: poloxamer 188, P20: polysorbate 20) are color-coded. Line types represent the results tested on various days after preparation.

poloxamer 188, or a combination of both). The obtained results further showed that lower concentrations of polysorbate 20 were necessary to achieve small particle sizes (Fig. 2) as compared to poloxamer 188 and especially when compared to the combination of both surfactants since a higher stabilization concentration was necessary to shift the particle size distribution of cinnarizine towards smaller size classes. Furthermore, it was observed that smaller sizes of cinnarizine particles were obtained when stabilized with polysorbate 20 (Fig. 2) with a stable distribution over 28 days. These observations correlated to the previous results explained by Zulbeari et al. (2024) which identified that lower concentrations in weight/volume percentage of polysorbate 20 were needed with regards to the surfactant coverage by a single surfactant molecule.

Further statistical tests were performed on the group milled with 1.0 mm beads to determine the significance of variables to the mean size (as characterized by D_{50}) and the size distribution (as characterized by span). As can be seen from Table 3, both the type of stabilizer ($p = 0.0047$) and its concentration ($p < 0.0001$) had significant influence on D_{50}, whereas no significance was found for the span (both $p > 0.05$). Pairwise t-tests with pooled data were performed to understand the role of concentration on D_{50} (Table 4). The significance letters categorized concentrations into four groups that had significant differences in mean

Table 4
A table summarizing the result of pairwise two-tailed t-tests with Bonferroni correction performed on 1.0 mm bead size group. The concentrations that do not share the significance letter represent a significant difference of mean D_{50} at 0.05 level.

Concentration (%)	Mean D_{50} (μm)	Significance Letter			
0.25	12.1	A	B		
0.50	14.3	A			
0.75	7.20			C	
1.00	8.40		B	C	
1.25	1.00				D
1.50	1.00				D
2.00	1.20				D
4.00	1.30				D

Table 3
Results of two-way ANOVA repeated measurements test after Greenhouse-Geisser correction performed on 1.0 mm bead size group.

Responses	Variables	Sum of Squares	Degrees of Freedom	Mean Square	F	Significance
D_{50} (μm)	Type of Stabilizer	1871.3	1.1	1675.1	26.31	0.0047
	Error(Type of Stabilizer)	284.5	4.5	63.7		
	Concentration (%)	3112.1	2.0	1581.4	49.75	0.0000
	Error(Concentration (%))	250.2	7.9	31.8		
	Type of Stabilizer * Concentration (%)	2688.5	2.0	1349.1	23.13	0.0005
	Error(Type of Stabilizer * Concentration (%))	465.0	8.0	58.3		
Span	Type of Stabilizer	1250.6	1.0	1245.2	2.22	0.2105
	Error(Type of Stabilizer)	2255.9	4.0	561.5		
	Concentration (%)	2367.1	1.1	2062.4	1.12	0.3542
	Error(Concentration (%))	8418.7	4.6	1833.8		
	Type of Stabilizer * Concentration (%)	4525.3	1.2	3926.6	1.04	0.3717
	Error(Type of Stabilizer * Concentration (%))	17327.2	4.6	3758.7		

D_{50} values in-between. It suggested that formulations prepared with concentrations above (and including) 1.25 % (significance letter group D) could achieve significantly smaller D_{50}, which was reflected by the change of mean D_{50} from the table. In addition, we highlight that for each type of stabilizer, this critical concentration is different, as these two factors (type of stabilizer and concentration) showed significant interaction ($p = 0.0005$). Further subgroup test results were enlisted in the Supplementary Materials in Table S1-3. These results implied that the stabilizer type and concentration had synergistic effects on the mean size of the prepared suspensions.

3.2. Quantifying unstable zone

Previous analysis had suggested the dependence of D_{50} on stabilizer type and concentration, using the 1.0 mm bead group as a representative example. However, it was still difficult to quantitatively define the unstable zone. Intuitively, if the size or size distribution changed over time, the formulation was referred to as 'unstable'. Therefore, the two characteristics D_{50} and span were examined. The standard deviation of D_{50} and span was calculated with respect to each formulation over the 4-week experimental period. The resulting D_{50}Std and SpanStd were believed to capture the suspension stability during the test. Similarly, means of D_{50} and Span were also calculated in a similar manner to serve as descriptions of each formulations' characteristics. Through such processing, the database was reduced to 72 points, each consisting of three variables: the type of stabilizer, concentration of the stabilizer, and bead size. From box plots (Fig. 3), the relationship between concentration and stability could be inferred. Focusing on the bottom two plots, which used standard deviation to depict the trend of Span and D_{50}, an increase in concentration was observed with enhanced stability. A higher concentration of stabilizers was also related to a narrower mean size and size distribution, as was seen in the top two plots of Fig. 3.

A scatter plot of SpanStd with D_{50}Std, alongside distribution plots of the two variables, were leveraged to quantitatively define the unstable zone (Fig. 4). As a low variance in D_{50} and Span was expected for stable formulations, the criteria that defined stability (represented as red lines) were proposed based on the histogram of D_{50}Std and SpanStd. More specifically, these lines were drawn at the valleys of the bimodal distributions. A standard deviation of 1.2 μm for the D_{50} over the experiment period was determined since two groups (with modes around 0.2 μm and 9.0 μm, respectively) could be observed from the histogram plotted at the top of Fig. 4. Similarly, the criterion of 1.8 for the span standard deviation was decided. Four quadrants were thus formed under the separation of these lines. Zone I was hereby defined as the stable zone, where the D_{50}Std SpanStd were below both criteria. To adhere to a strict definition of physical stability, formulations that produced results in Zone II were considered as unstable for a drifting D_{50}. In Zone III, the variation of Span went over the threshold, indicating a changing particle

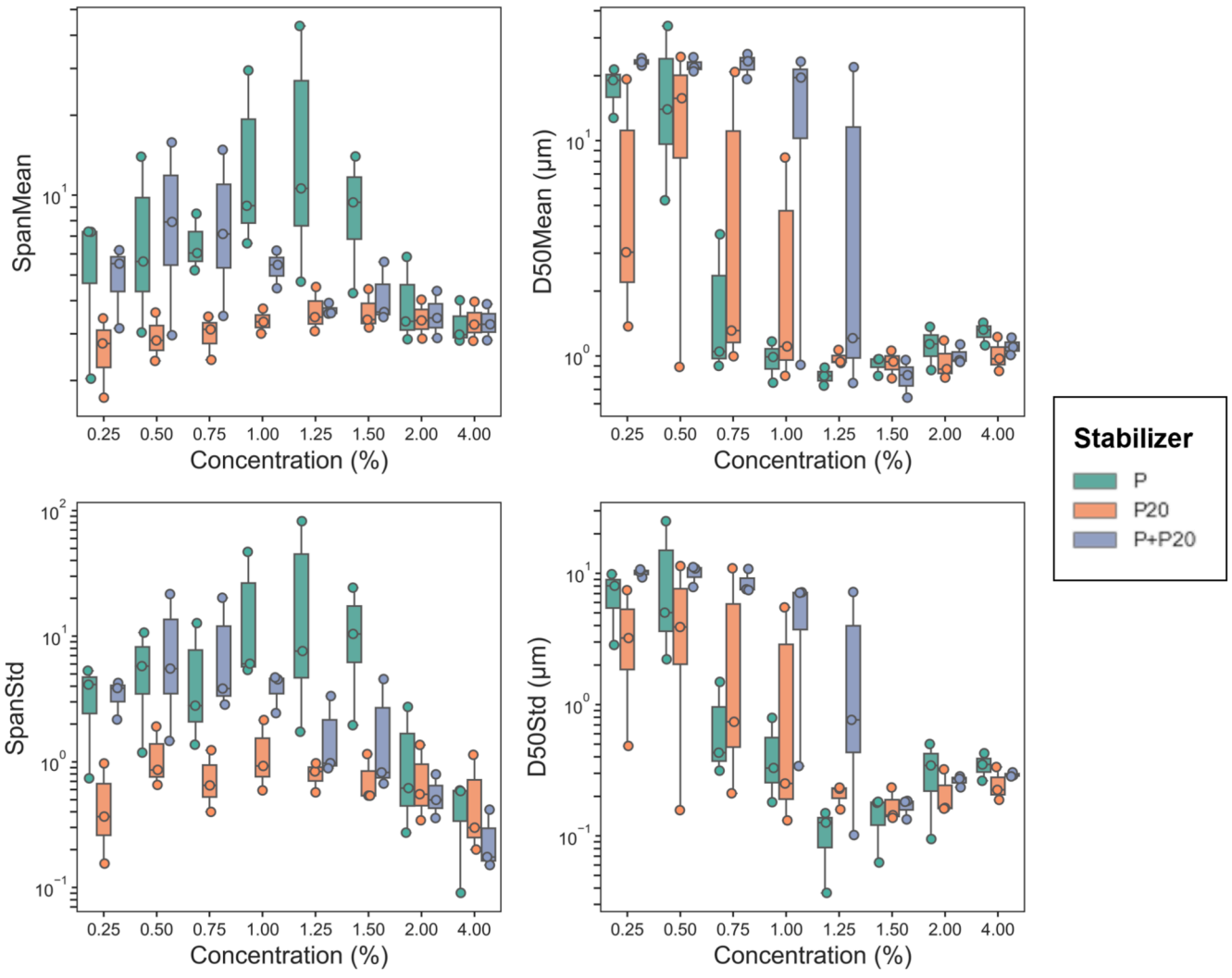

Fig. 3. Box plots of SpanMean, SpanStd, D_{50}Mean, and D_{50}Std with respect to the concentration of stabilizers (0.25% to 4.00% w/v). The stabilizer type (P: poloxamer 188, P20: polysorbate 20) was color-coded. The three dots in each box were samples prepared from three different bead sizes.

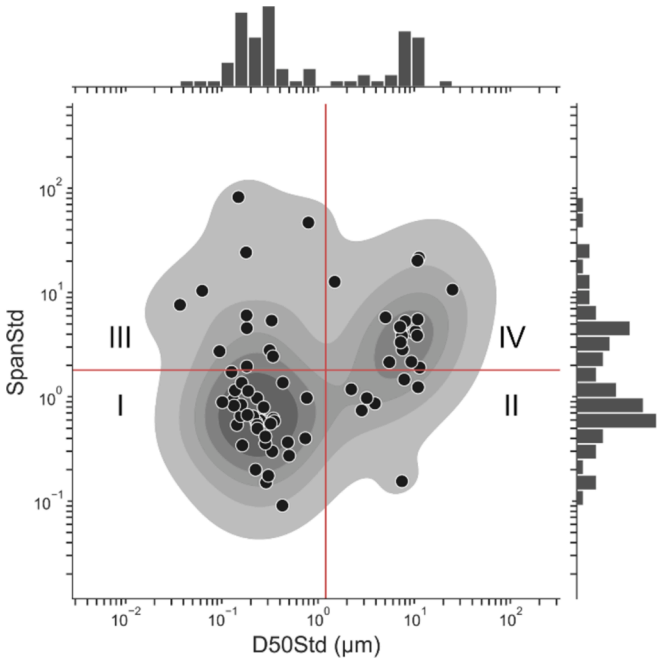

Fig. 4. A scatter plot showing SpanStd against D_{50}Std with each dot represents one formulation. The underlying contours were generated by KDE to assist visualization. On the side the distribution plots are drawn. The red lines define four quadrants in the plot, in which zone I was regarded as the stable zone. (For interpretation of the references to color in this figure legend, the reader is referred to the web version of this article.)

size distribution due to the formation of larger particle clusters which expanded the span. In zone IV, both D_{50} and Span of the formulation increased and was considered as unstable.

To confirm the validity of the cut-offs for the stable/unstable zone, unsupervised learning algorithms were applied to rule out potential clusters within the data. More specifically, k-means clustering and GMM were applied to the data from Fig. 4. The results of clustering could be found in Figure S4, revealing a very similar choice of zones. Furthermore, pair-wise Cohen's Kappa was introduced to quantitatively measure the similarity between the empirically drawn cut-offs and the algorithm-generated clusters. Cohen's Kappa for human vs. k-means and human vs. GMM was calculated as 0.972 and 0.889, respectively. As a reference, the value between the two unsupervised learning algorithms was 0.916. As reported previously, a Kappa value above 0.8 indicated strong agreement between different voters (McHugh, 2012). Therefore, these results helped justify the selection of partitioning cut-offs to effectively separate stable and unstable formulations for further ML modelling.

3.3. Classification with Machine learning models

With the stability labels available, ML models were constructed to help predict the stability of formulations based on the bead size, stabilizer type and concentration (Fig. 5). Overall, the training set was balanced with 35 stable formulations and 37 unstable formulations according to the threshold. Multiple algorithms with diverse modelling mechanisms were attempted and benchmarked to identify the most suitable one for the stability modelling task. After hyperparameter optimization, all classifiers were benchmarked based on the accuracy and F_1 score metrics. Interestingly, the performance was similar for both metrics, indicating a relativity simple classification task. In particular, the XGBoost model succeeded with a slight edge on the mean of accuracy (0.91 ± 0.11) and F_1 score (0.91 ± 0.09) within the 10-fold cross validation process. Through inspecting the confusion matrix of the XGBoost model, the prediction accuracy was satisfactory on both

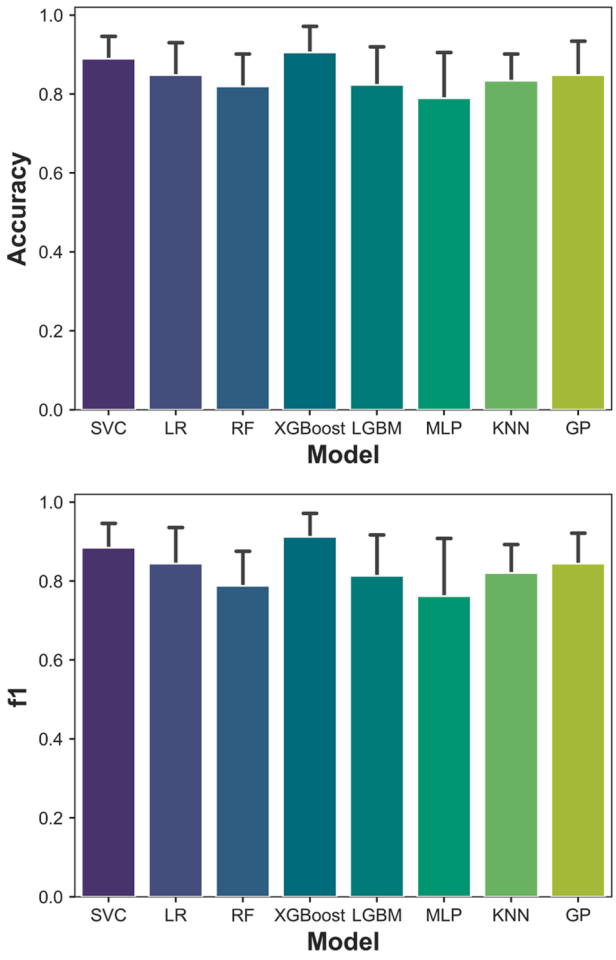

Fig. 5. Classification performance of various machine learning models under their optimized hyperparameters. The error bars come from 10-fold cross validation.

training and test sets (Fig. 6). The superior performance of XGBoost models was also confirmed in other studies that modelled small and tabular datasets (Tao et al., 2021; Wang et al., 2022). In fact, the tree-based algorithm that XGBoost relied on was considered efficient and highly compatible with variables, making it a popular option for modelling complicated relationships in materials and pharmaceutics research (Wu et al., 2017). The capacity to handle missing values also gave it an edge in future deployment as a predictive tool. Overall, it was decided to proceed with the XGBoost model for further model interpretation.

3.4. Model interpretation

The trained XGBoost model was explained through SHAP analysis. Different from conventional model interpretation strategies, SHAP benefited from game theory and could provide insight into the positive/negative contribution of variables to the final prediction result (Lundberg et al., 2020). Here, SHAP analysis was leveraged to understand the modelling result produced with XGBoost (Fig. 7). From two examples of an unstable and a stable prediction presented in Fig. 7(a) and (b), it was clearly observed that using P (poloxamer 188) as the stabilizer was detrimental for the stabilization (compared with other stabilizers). This coincided with the observation from Fig. 3, where most suspensions stabilized with poloxamer 188 showed high variation in D_{50} and Span. The positive (stable) sample in Fig. 7(b) showed that with a high concentration, the impact of stabilizer became negligible for the prediction results. The overall analysis showed that concentration as a

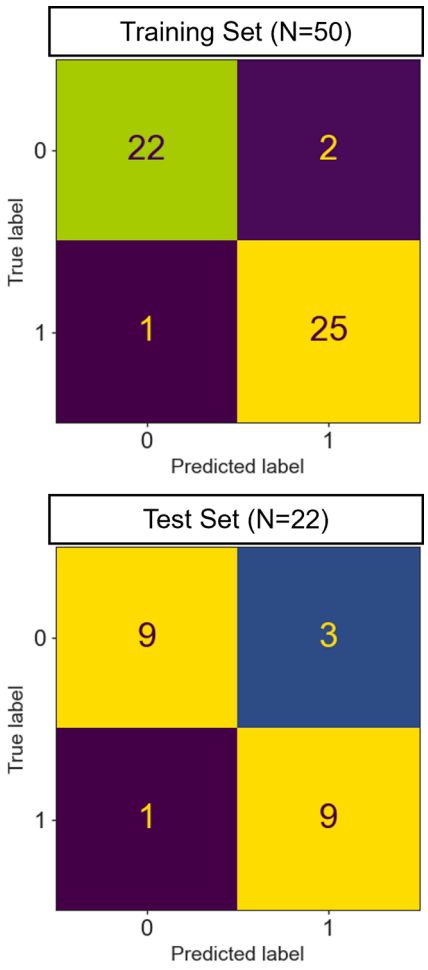

Fig. 6. The confusion matrix for the XGBoost model under 67%/33% partitioning of the full dataset.

variable was indeed the most important feature during the prediction process of the ML classifier, whereas the bead size as a variable had a lower impact based on the analysis compared to the stabilizer concentration. The analysis showed that a higher bead size contributed towards a stable prediction for all data, as reflected by the positive SHAP values assigned to bead sizes of 1.0 and 0.8 mm in Fig. 7c. This could further correlate to the general understanding of the bead size effect where the usage of larger bead sizes typically leads to larger sizes of drug particles and by that means, towards a more thermodynamic stable system. Compared to systems where smaller drug particles are obtained, the total surface area and interfacial tension between solid drug particles and the aqueous dispersion medium is increased and particles tend to irreversibly aggregate in an attempt to reduce the free energy (Lestari et al., 2015). Thereby, it would ultimately lead towards a more physically unstable formulation if not stabilized sufficiently.

So far, the impact of concentration and bead size have been discussed. The following section placed the focus on the stabilizer. Having polysorbate 20 as the stabilizer positively contributed to the model towards a stable prediction. An interesting finding from the model was that the combination of polysorbate 20 and poloxamer 188 was not helpful for the stabilization of the formulation, even though polysorbate 20 alone was shown to be effective as a stabilizer. The combination of multiple stabilizers has, in some cases, been favorable due to enhanced long-term stability (Peltonen & Hirvonen, 2010). However, based on the obtained ML results in the present study, the stability of the prepared cinnarizine suspensions would not benefit from the combination of poloxamer 188 and polysorbate 20, since the model predicted that polysorbate 20 alone was more efficient with lower stabilization concentrations necessary rather when combining the two non-ionic surfactants. By this, the addition of poloxamer 188 to polysorbate 20 seemed to have a negative impact on the sizes of cinnarizine particles, detaining the most stable formulation system. These findings were in good accordance with the experimental data on the physical properties of the individual surfactants with regards to the short-term stress physical stability investigated by particle size profiles as a function of time. The experimental data showed that physical stable formulations were first obtained at higher concentrations of stabilizer when polysorbate 20 and poloxamer 188 were combined as for the surfactants individually, supporting the ML findings. The *d*-values of cinnarizine

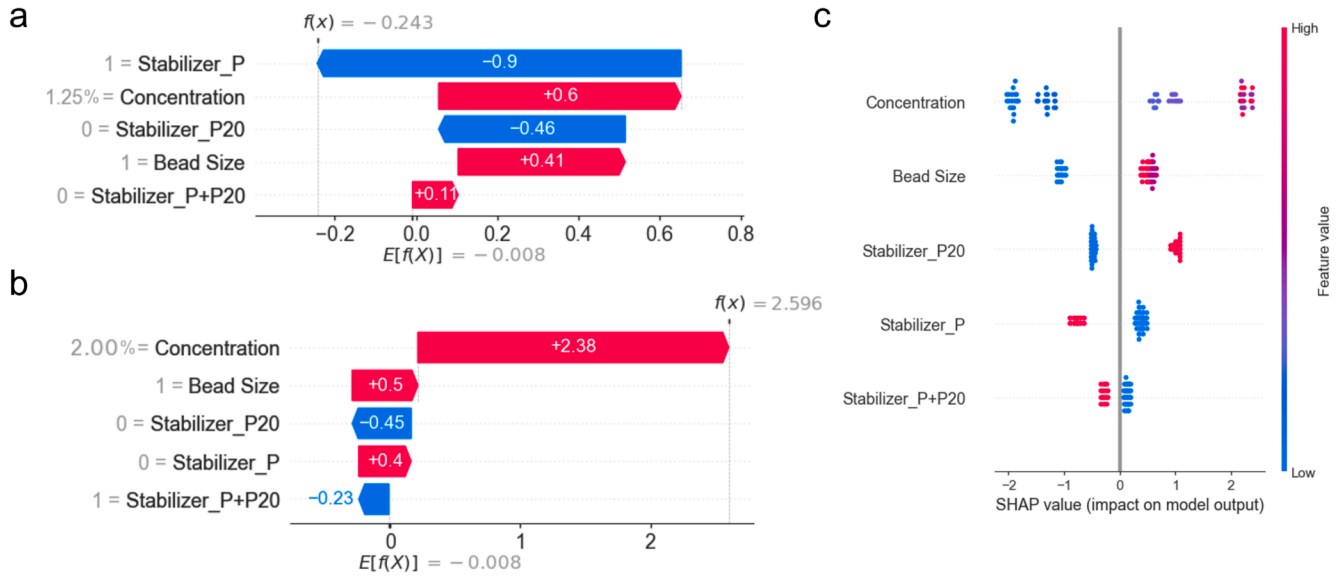

Fig. 7. SHAP Analysis results from the XGBoost model trained from the stability dataset. (a) The contribution of variables in the prediction of an unstable formulation. (b) The contribution of variables in the prediction of a stable formulation. (c) An overview of feature value in the prediction process (ranked from top to bottom).

suspensions stabilized with a combination of polysorbate 20 and poloxamer 188 can be found in the Supplementary Materials (Table S4-S6). From a formulation perspective, the combination of the two surfactants would therefore not benefit the stabilization of suspensions containing cinnarizine as the model drug based on both the experimental data and the ML algorithms.

By this, a good agreement was observed between the ML-based prospect and the experimental observations. ML-based approach was linked to suspension research by obtaining insights about stability and formulation variables quantitatively through model interpretation. In addition, the predictive aspect of the ML model could benefit the research of LAIs by providing the stability information much faster than the laboratory-based stability testing over a month. Nevertheless, ML only extracts phenomenological relationships from data, and more detailed mechanistic studies of microsuspension formulations will be needed to cross-validate and explain the obtained conclusions. In the present study the foundation for microsuspension formulation stability prediction was laid. Future works are required to expand this model to accommodate more APIs and stabilizers, contributing to a more generalizable model for broader pharmaceutical applications.

4. Conclusion

In summary, this study leveraged ML algorithms to assist the formulation design of pharmaceutical suspensions. The XGBoost model, trained on formulation parameters, yielded high prediction accuracy on the long-term stability of suspensions. Model interpretation provided further insights in the formulation process. For the selection of stabilizer, polysorbate 20 stood out for its positive contribution towards a stable prediction in ML compared with poloxamer 188. Furthermore, no synergistic effect was observed from combining the two surfactants during preparation on the stabilization capacity. In addition, statistical analysis showed nanosuspension characteristics, such as their size and size distribution, were significantly influenced by the concentration of the stabilizer, followed by the bead size. These data-driven modelling results correlated well with mechanistic analysis. Through the present study, a predictive model was established from full factorial experiments and insights for cinnarizine suspension formulation were gained through model interpretation to assist the formulation of cinnarizine nano- and microsuspensions. We also highlight this pipeline combining traditional statistical analysis, explainable ML, and mechanistic analysis as a new paradigm to empower future LAI research.

CRediT authorship contribution statement

Nadina Zulbeari: Writing – original draft, Formal analysis, Data curation, Conceptualization. **Fanjin Wang:** Writing – original draft, Visualization, Formal analysis, Data curation, Conceptualization. **Sibel Selyatinova Mustafova:** Writing – review & editing, Data curation. **Maryam Parhizkar:** Writing – review & editing, Supervision, Methodology, Conceptualization. **René Holm:** Writing – review & editing, Supervision, Resources, Project administration, Methodology, Funding acquisition, Conceptualization.

Declaration of competing interest

The authors declare that they have no known competing financial interests or personal relationships that could have appeared to influence the work reported in this paper.

Appendix A. Supplementary material

Supplementary data to this article can be found online at https://doi.org/10.1016/j.ijpharm.2024.124967.

Data availability

Data will be made available on request.

References

Alidori, S., Subramanian, R., Holm, R., 2024. Patient-centric long-acting injectable and implantable platforms—an industrial perspective. *Mol. Pharm.* 21 (9), 4238–4258. https://doi.org/10.1021/acs.molpharmaceut.4c00665.

Azad, M., Afolabi, A., Bhakay, A., Leonardi, J., Davé, R., & Bilgili, E. (2015). Enhanced physical stabilization of fenofibrate nanosuspensions via wet co-milling with a superdisintegrant and an adsorbing polymer. *European journal of pharmaceutics and biopharmaceutics : official journal of Arbeitsgemeinschaft fur Pharmazeutische Verfahrenstechnik e.V*, *94*, 372–385. doi: 10.1016/j.ejpb.2015.05.028.

Bannigan, P., Aldeghi, M., Bao, Z., Häse, F., Aspuru-Guzik, A., Allen, C., 2021. Machine learning directed drug formulation development. Adv Drug Deliv Rev. 175, 113806. https://doi.org/10.1016/j.addr.2021.05.016. Epub 2021 May 19 PMID: 34019959.

Bannigan, P., Bao, Z., Hickman, R.J., Aldeghi, M., Häse, F., Aspuru-Guzik, A., Allen, C., 2023. Machine learning models to accelerate the design of polymeric long-acting injectables. Nat Commun. 14 (1), 35. https://doi.org/10.1038/s41467-022-35343-w. PMID: 36627280; PMCID: PMC9832011.

Bao, Q., Zou, Y., Wang, Y., Choi, S., Burgess, D.J., 2021. Impact of Formulation Parameters on In Vitro Release from Long-Acting Injectable Suspensions. *AAPS J.* 23 (2), 42. https://doi.org/10.1208/s12248-021-00566-0.

Bauer, A., Berben, P., Chakravarthi, S.S., Chattorraj, S., Garg, A., Gourdon, B., Heimbach, T., Huang, Y., Morrison, C., Mundhra, D., Palaparthy, R., Saha, P., Siemons, M., Shaik, N.A., Shi, Y., Shum, S., Thakral, N.K., Urva, S., Vargo, R., Koganti, V.R., Barrett, S.E., 2023. Current State and Opportunities with Long-acting Injectables: Industry Perspectives from the Innovation and Quality Consortium "Long-Acting Injectables" Working Group. *Pharmaceutical Research* 40 (7), 1601–1631. https://doi.org/10.1007/s11095-022-03391-y.

Bitterlich, A., Laabs, C., Krautstrunk, I., Dengler, M., Juhnke, M., Grandeury, A., Bunjes, H., & Kwade, A. (2015). Process parameter dependent growth phenomena of naproxen nanosuspension manufactured by wet media milling. *European journal of pharmaceutics and biopharmaceutics : official journal of Arbeitsgemeinschaft fur Pharmazeutische Verfahrenstechnik e.V*, *92*, 171–179. doi: 10.1016/j.ejpb.2015.02.031.

Choi, J.Y., Yoo, J.Y., Kwak, H.S., Nam, B.U., Lee, J., 2005. Role of polymeric stabilizers for drug nanocrystal dispersions. J. Curr. Appl. Phys. 5, 472–474. https://doi.org/10.1016/j.cap.2005.01.012.

De Cleyn, E., Holm, R., Van den Mooter, G., 2019. Size analysis of small particles in wet dispersions by laser diffractometry: a guidance to quality data. *J. Pharm. Sci.* 108 (5), 1905–1914. https://doi.org/10.1016/j.xphs.2018.12.010.

Ferrar, J.A., Sellers, B.D., Chan, C., Leung, D.H., 2020. Towards an improved understanding of drug excipient interactions to enable rapid optimization of nanosuspension formulations. *Int. J. Pharm.* 578, 119094. https://doi.org/10.1016/j.ijpharm.2020.119094.

U.S. Food and Drug Administration. (2024). Drug Approvals and Databases. Inactive Ingredient Search for Approved Drug Products Search. Available at: https://www.accessdata.fda.gov/scripts/cder/iig/index.cfm. Accessed online: 10-05-2024.

George, M., Ghosh, I., 2013. Identifying the correlation between drug/stabilizer properties and critical quality attributes (CQAs) of nanosuspension formulation prepared by wet media milling technology. *European Journal of Pharmaceutical Sciences : Official Journal of the European Federation for Pharmaceutical Sciences* 48 (1–2), 142–152. https://doi.org/10.1016/j.ejps.2012.10.004.

Guner, G., Mehaj, M., Seetharaman, N., Elashri, S., Yao, H.F., Clancy, D.J., Bilgili, E., 2023. Do Mixtures of Beads with Different Sizes Improve Wet Stirred Media Milling of Drug Suspensions? *Pharmaceutics* 15 (9), 2213. https://doi.org/10.3390/pharmaceutics15092213.

Hagedorn, M., Bögershausen, A., Rischer, M., Schubert, R., Massing, U., 2017. Dual centrifugation - A new technique for nanomilling of poorly soluble drugs and formulation screening by an DoE-approach. *Int. J. Pharm.* 530 (1–2), 79–88. https://doi.org/10.1016/j.ijpharm.2017.07.047.

Holm, R., Lee, R.W., Glassco, J., DiFranco, N., Bao, Q., Burgess, D.J., Lukacova, V., Alidori, S., 2023. Long acting injectable aqueous suspensions – summary from an AAPS workshop. AAPS J. 25, 49.

Karakucuk, A., Celebi, N., 2020. Investigation of Formulation and Process Parameters of Wet Media Milling to Develop Etodolac Nanosuspensions. *Pharm. Res.* 37 (6), 111. https://doi.org/10.1007/s11095-020-02815-x.

Kipp, J.E., 2004 Oct 13. The role of solid nanoparticle technology in the parenteral delivery of poorly water-soluble drugs. Int J Pharm. 284 (1–2), 109–122. https://doi.org/10.1016/j.ijpharm.2004.07.019. PMID: 15454302.

Lee, J., Choi, J.Y., Park, C.H., 2008. Characteristics of polymers enabling nano-comminution of water-insoluble drugs. *International Journal of Pharmaceutics* 355 (1–2), 328–336. https://doi.org/10.1016/j.ijpharm.2007.12.032.

Lestari, M.L., Müller, R.H., Möschwitzer, J.P., 2015. Systematic screening of different surface modifiers for the production of physically stable nanosuspensions. *J. Pharm. Sci.* 104 (3), 1128–1140. https://doi.org/10.1002/jps.24266.

Li, M., Azad, M., Davé, R., Bilgili, E., 2016. Nanomilling of Drugs for Bioavailability Enhancement: A Holistic Formulation-Process Perspective. *Pharmaceutics* 8 (2), 17. https://doi.org/10.3390/pharmaceutics8020017.

Lundberg, S.M., Erion, G., Chen, H., DeGrave, A., Prutkin, J.M., Nair, B., Katz, R., Himmelfarb, J., Bansal, N., Lee, S.I., 2020. From Local Explanations to Global

Understanding with Explainable AI for Trees. *Nat. Mach. Intell.* 2 (1), 56–67. https://doi.org/10.1038/s42256-019-0138-9.

McHugh, M.L., 2012. Interrater reliability: the kappa statistic. *Biochemia Medica* 22 (3), 276–282. https://doi.org/10.11613/bm.2012.031.

Mishra, B., Sahoo, J., Dixit, P.K., 2015. Formulation and process optimization of naproxen nanosuspensions stabilized by hydroxy propyl methyl cellulose. *Carbohydr. Polym.* 127, 300–308. https://doi.org/10.1016/j.carbpol.2015.03.077.

Muller, R.H., Keck, C.M., 2004. *J. Biotechnol.* 113 (1–3), 151–170. https://doi.org/10.1016/j.jbiotec.2004.06.007.

Nakach, M., Authelin, J.R., Tadros, T., Galet, L., Chamayou, A., 2014. Engineering of nano-crystalline drug suspensions: employing a physico-chemistry based stabilizer selection methodology or approach. *Int. J. Pharm.* 476 (1–2), 277–288. https://doi.org/10.1016/j.ijpharm.2014.09.048.

Nakach, M., Authelin, J.R., Voignier, C., Tadros, T., Galet, L., Chamayou, A., 2016. Assessment of formulation robustness for nano-crystalline suspensions using failure mode analysis or derisking approach. *Int. J. Pharm.* 506 (1–2), 320–331. https://doi.org/10.1016/j.ijpharm.2016.04.043.

Nkanga, C.I., Fisch, A., Rad-Malekshahi, M., Romic, M.D., Kittel, B., Ullrich, T., Wang, J., Krause, R.W.M., Adler, S., Lammers, T., Hennink, W.E., Ramazani, F., 2020. Clinically established biodegradable long acting injectables: An industry perspective. *Adv. Drug Deliv. Rev.* 167, 19–46. https://doi.org/10.1016/j.addr.2020.11.008.

Okoli, C.T.C., Kappi, A., Wang, T., Makowski, A., Cooley, A.T., 2022. The effect of long-acting injectable antipsychotic medications compared with oral antipsychotic medications among people with schizophrenia: A systematic review and meta-analysis. *Int. J. Ment. Health Nurs.* 31 (3), 469–535. https://doi.org/10.1111/inm.12964.

Owen, A., Rannard, S., 2016. Strengths, weaknesses, opportunities and challenges for long acting injectable therapies: Insights for applications in HIV therapy. *Adv. Drug Deliv. Rev.* 103, 144–156. https://doi.org/10.1016/j.addr.2016.02.003.

Pacchiarotti, I., Tiihonen, J., Kotzalidis, G.D., Verdolini, N., Murru, A., Goikolea, J.M., Valentí, M., Aedo, A., Vieta, E., 2019. Long-acting injectable antipsychotics (LAIs) for maintenance treatment of bipolar and schizoaffective disorders: A systematic review. *Eur. Neuropsychopharmacol.* 29 (4), 457–470. https://doi.org/10.1016/j.euroneuro.2019.02.003.

Park, E.J., Amatya, S., Kim, M.S., Park, J.H., Seol, E., Lee, H., Shin, Y.H., Na, D.H., 2013. Long-acting injectable formulations of antipsychotic drugs for the treatment of schizophrenia. *Arch. Pharm. Res.* 36 (6), 651–659. https://doi.org/10.1007/s12272-013-0105-7.

Peltonen, L., Hirvonen, J., 2010. Pharmaceutical nanocrystals by nanomilling: critical process parameters, particle fracturing and stabilization methods. *J. Pharm. Pharmacol.* 62 (11), 1569–1579. https://doi.org/10.1111/j.2042-7158.2010.01022.x.

Tao, H., Wu, T., Aldeghi, M., Wu, T.C., Aspuru-Guzik, A., Kumacheva, E., 2021. Nanoparticle synthesis assisted by machine learning. *Nat. Rev. Mater.* 6, 701–716. https://doi.org/10.1038/s41578-021-00337-5.

Vamathevan, J., Clark, D., Czodrowski, P., Dunham, I., Ferran, E., Lee, G., Li, B., Madabhushi, A., Shah, P., Spitzer, M., Zhao, S., 2019. Applications of machine learning in drug discovery and development. *Nat. Rev. Drug Discov.* 18 (6), 463–477. https://doi.org/10.1038/s41573-019-0024-5.

Van Eerdenbrugh, B., Vermant, J., Martens, J.A., Froyen, L., Van Humbeeck, J., Augustijns, P., Van den Mooter, G., 2009. A screening study of surface stabilization during the production of drug nanocrystals. *J. Pharm. Sci.* 98 (6), 2091–2103. https://doi.org/10.1002/jps.21563.

Verma, S., Gokhale, R., Burgess, D.J., 2009. A comparative study of top-down and bottom-up approaches for the preparation of micro/nanosuspensions. *Int. J. Pharm.* 380 (1–2), 216–222. https://doi.org/10.1016/j.ijpharm.2009.07.005.

Verma, S., Kumar, S., Gokhale, R., Burgess, D.J., 2011. Physical stability of nanosuspensions: investigation of the role of stabilizers on Ostwald ripening. *Int. J. Pharm.* 406 (1–2), 145–152. https://doi.org/10.1016/j.ijpharm.2010.12.027.

Wang, F., Elbadawi, M., Tsilova, S.L., Gaisford, S., Basit, A.W., Parhizkar, M., 2022. Machine learning predicts electrospray particle size. *Mater. Des.* 219, 110735. https://doi.org/10.1016/j.matdes.2022.110735.

Wilkinson, J., Ajulo, D., Tamburrini, V., Gall, G.L., Kimpe, K., Holm, R., Belton, P., Qi, S., 2022. Lipid based intramuscular long-acting injectables: Current state of the art. *Eur. J. Pharm. Sci.* 178, 106253. https://doi.org/10.1016/j.ejps.2022.106253.

Willmann, A.C., Berkenfeld, K., Faber, T., Wachtel, H., Boeck, G., Wagner, K.G., 2022. Itraconazole nanosuspensions via dual centrifugation media milling: impact of formulation and process parameters on particle size and solid-state conversion as well as storage stability. *Pharmaceutics* 14 (8), 1528. https://doi.org/10.3390/pharmaceutics14081528.

Wu, Z., Ramsundar, B., Feinberg, E.N., Gomes, J., Geniesse, C., Pappu, A.S., Leswing, K., Pande, V., 2017. MoleculeNet: a benchmark for molecular machine learning. *Chem. Sci.* 9 (2), 513–530. https://doi.org/10.1039/c7sc02664a.

Zulbeari, N., Mustafova, S.S., Simonsen, A.C., Lund, F.W., Holm, R., 2024. The Langmuir-Blodgett trough (Langmuir film balance) can be used to understand the stabilizer concentrations in aqueous nano- and microsuspensions. *Int. J. Pharm.* 665, 124726. https://doi.org/10.1016/j.ijpharm.2024.124726.